

Carbonization of Lignin Extracted from Liquid Waste of Coconut Coir Delignification

Widiyastuti Widiyastuti^{1,*}, Mahardika Fahrudin Rois¹, Heru Setyawan¹,
Siti Machmudah¹, and Diky Anggoro²

¹Department of Chemical Engineering, Institut Teknologi Sepuluh Nopember, Kampus ITS Sukolilo, Surabaya 60111, Indonesia

²Department of Physics, Institut Teknologi Sepuluh Nopember, Kampus ITS Sukolilo, Surabaya 60111, Indonesia

* **Corresponding author:**

tel: +62-31-5946240

email: widi@chem-eng.its.ac.id

Received: June 10, 2019

Accepted: October 14, 2019

DOI: 10.22146/ijc.46484

Abstract: Lignin, as a by-product of the pulping process, is less widely used for worth materials. In this study, the utilization of lignin by-product of the soda delignification process of coconut coir converted to the activated carbon by a simple precipitation method followed by the carbonization at various temperatures is presented. The by-product liquor of the soda delignification process having a pH of 13.4 was neutralized by dropping of hydrochloric acid solution to achieve the pH solution of 4, resulting in the lignin precipitation. The precipitated was washed, filtered, and dried. The dried lignin was then carbonized under a nitrogen atmosphere at various temperatures of 500, 700, and 900 °C. The dried lignin and carbonized samples were characterized using SEM, XRD, FTIR, and nitrogen adsorption-desorption analyzer, to examine their morphology, X-Ray diffraction pattern, chemical bonding interaction, and surface area-pore size distribution, respectively. The characterization results showed that the functional groups of lignin mostly disappeared gradually with the increase of temperature approached the graphite spectrum. The XRD patterns confirmed that the carbonized lignin particles were amorphous and assigned as graphitic. All samples had a pore size of 3–4 nm classified as mesoporous particles. This study has shown that the carbonization lignin at a temperature of 700 °C had the highest surface area (i.e., 642.5 m²/g) in which corresponds to the highest specific capacitance (i.e., 28.84 F/g).

Keywords: coconut coir; soda delignification; lignin; carbonization; mesoporous particles

■ INTRODUCTION

Lignin is the most abundant renewable source of aromatic groups in nature and the second most abundant terrestrial biopolymer after cellulose. The pulp and paper industry is the primary producer of cellulose-rich fibers. Besides, cellulosic ethanol facilities are currently coming to resolve the limitation of fossil fuel. Both industries produce lignin as a by-product. The processes of Kraft, sulfite, soda, organosolv, and hydrothermal are some of the delignification methods that use sodium hydroxide and sodium sulfide, sulfur dioxide, sodium hydroxide, an organic solvent, and highly compressed water and temperature, respectively, to separate cellulose fiber by dissolving the lignin. For non-woody lignocellulose sources, soda pulping is widely used for the delignification method [1].

On the other hand, the lignin market is still limited for the valuable application [2]. Therefore, the conversion of lignin to the more valuable functional materials is still a challenge, even though lignin is becoming promising for many future applications [3-5]. As the by-product, lignin liquor is usually treated as liquid wastewater, and then it is concentrated and fired to serve only as fuel producing steam, electricity, and inorganic chemical for internal mill use [6]. Several efforts for extracting lignin from black liquor before further processing are membrane-assisted electrochemical [7] and precipitation through the addition of an acidifying agent of carbon dioxide [8], chloric acid [9], and sulfuric acid [10].

Carbon black is mostly produced from incomplete combustion of fossil fuel. The utilization of agricultural

bio-waste materials directly without separating the components of the bio-waste materials that contain cellulose, hemicellulose, and lignin has also been used for activated carbon sources [11]. The cellulose is separated from lignin for the use of the biofuel process. The utilization of lignin itself to produce carbon black has been attempted, but it is still limited. Macroporous carbon was prepared from lignin by using poly(methyl methacrylate) as the template [12]. Usually, phenolic resin and polystyrene latex were used as the carbon source and template particles, respectively, to generate macroporous carbon nanospheres [13]. The use of lignin from bioethanol co-product using the hydrolysis process for conductive carbon black filler has been studied [14]. Powdered and granular carbon adsorbents are also produced from hydrolysis lignin as the by-product of biofuels [15]. The highest specific surface area was 654 m²/g obtained from the lignin carbonization at a temperature of 900 °C, followed by ball milling. Activated carbon from commercial alkali lignin was synthesized by simultaneous carbonization and alkali hydroxide activation for supercapacitors application [16]. The use of lignin sources and lignin-rich biomass were also compared to the effects of the carbonization process on the activated carbon properties [17]. Alkali lignin purified from papermaking black-liquor was also used to generate a composite of carbon/ZnO for the photocatalytic application [18]. Biomass-based lignin extracted from industrial waste black liquor was carbonized and activated by steam to produce activated carbon [10]. Most of them use lignin from the delignification of wood source, notably pulp and mill industry. Lack of them use non-wood source, and as far as our knowledge, none of them use lignin from the delignification process of coconut coir. The study is needed because different raw material and activation procedure plays an essential role in the characteristics of the generated activated carbon. The microstructure, structure, and electrical characteristics of carbonaceous materials are highly influenced by the lignin feedstock [19].

In this study, the carbonization of lignin extracted from the liquor of coconut coir delignification using the soda-pulping process was introduced with simple precipitation and calcination methods. The effect of the

temperature of carbonization on the characteristics of the generated particles was elucidated. The samples were characterized using scanning electron microscopy (SEM), X-Ray diffraction (XRD), Fourier transform infrared spectrometry (FTIR), and nitrogen adsorption-desorption analyzer to examine the best condition for lignin carbonization derived from coconut coir. The specific capacitance was also measured from the cyclic voltammetry (CV) curve and the correlation with the other particle characteristics was studied.

■ EXPERIMENTAL SECTION

Materials

The liquor obtained from the delignification of coconut coir for cellulose aerogel preparation by the soda process with a pH of 13.4 was used as raw material [20]. The coconut coir was obtained from a traditional market in Keputih, Surabaya, Indonesia. Hydrochloric acid (HCl) 37 wt.% in analytical grade was purchased from Merck.

Instrumentation

The instrumentation used for samples' characterizations were thermogravimetric and differential analysis (TG-DTA, Shimadzu DTG-60H), X-Ray diffraction (XRD, PanAnalytical X'Pert MPD System), Fourier transform infrared spectroscopy (FTIR, Nicolet iS10), scanning electron microscopy (SEM, Hitachi FlexSEM 1000), a nitrogen adsorption-desorption analyzer (Nova 1200e, Quantachrome), and a potentiostat/galvanostat instrument (Metrohm, Autolab PGSTAT302N).

Procedure

Sample preparation

A solution of 1.5 M HCl prepared from HCl 37 wt.% was added drop by drop into the raw material under stirring to decrease the pH liquor of 4 and to precipitate the lignin. The precipitated particles were separated from the liquid by centrifugation and washed ten times to ensure the salt formed did not contaminate the extracted lignin. The precipitated particles were filtered and then dried in the oven at a temperature of 80 °C for 12 h. The dried lignin was calcined in the furnace under the flow of nitrogen with a flow rate of 100 mL/min.

For the sample of carbonized lignin at 500 °C, the dried lignin was gradually heated from 100 °C for 30 min, then at 300 °C for 1 h, and then at 500 °C for 2 h. For the samples of carbonized lignin at 700 and 900 °C, the preliminary treatment was the same with the sample of carbonized lignin 500 °C, and the next step was to continue heating at 700 and 900 °C, respectively, for 2 h.

Sample characterizations

Simultaneous measurement of thermogravimetric and differential analysis was used to examine the weight losses due to lignin decomposition by increasing the temperature. The heating rate was 5 °C/min under the flow of nitrogen. X-Ray diffraction with Cu K α as the radiation source ($\lambda = 0.15406$ nm) was used to evaluate the microstructure of the generated particles. Fourier transform infrared spectroscopy was used to characterize the functional group of the samples. Scanning electron microscopy was used to investigate the morphology of the generated particles. A nitrogen adsorption-desorption analyzer measured at 77 K, the boiling point of nitrogen, was used for surface area and pore characterization. The samples were degassed under the flow of nitrogen at 300 °C for 3 h. The total pore volume of the samples was estimated from the adsorption branch of the isotherm at a relative pressure P/P_0 close to 1. The specific surface area of the samples was calculated by using the multiple-point Brunauer-Emmett-Teller (BET) method at $P/P_0 < 0.3$. The pore size distribution of the samples at the adsorption isotherm using the Barret-Joyner-Halenda (BJH) method was used to determine the diameter and volume of pore samples. The specific capacitance was determined from cyclic voltammetry (CV) at potential applied ranging from -1 to 0 V with a sweep rate of 10 mV/sec using potentiostat/galvanostat instrument. The sample was prepared by mixing the carbon sample and polyvinylidene difluoride (PVdF) at a ratio of 10:1 by weight and transforming the mixture into carbon paste by adding drops of 1-methyl-2-pyrrolidone (NMP). The paste was coated to 1.5 cm² nickel-foam assigned as a working electrode. A platinum foil and Ag/AgCl electrode were used as the counter and reference electrodes, respectively. 100 mL of 0.1 M Na₂S₂O₃ was used as an

electrolyte solution. The specific capacitance (C_s , F/g) was calculated using the following equation:

$$C_s = \frac{1}{mv(V_c - V_a)} \int_{V_a}^{V_c} I(V) dV \quad (1)$$

where v is the potential scan rate (mV/sec), $(V_c - V_a)$ is the applied potential range (V), I is the current response per unit area (mA/cm²), and m is the mass of a sample (g).

RESULTS AND DISCUSSION

The Composition and the Thermal Analysis of the Dried Lignin

The proximate analysis of dried lignin indicated that the volatile matter has the highest composition of 38.03 wt.%, followed by fixed carbon as the second-highest composition of 37.00 wt.%. The ash and the moisture contents of the dried lignin were 21.06 and 3.91 wt.%, respectively. The proximate analysis was supported by gravimetric analysis under the flow of nitrogen, as shown in Fig. 1. The first peak on the DTA graph corresponds to the loss of around 4.5 wt.% moisture content at around 100 °C as indicated by the TG graph. The second peak of the DTA graph occurred at around 416 °C corresponds to around 37 wt.% loss of volatile compounds in the lignin. The clear peak does not indicate the loss of carbon on the DTA graph because of the slow degradation rate of carbon up to the temperature at around 860 °C with the remaining weight at around 21.6 wt.% corresponds to the ash content.

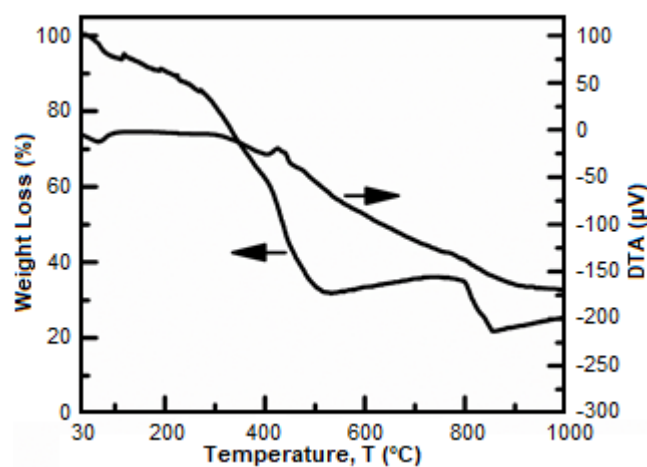


Fig 1. Thermogravimetric analysis of dried lignin using under the flow of nitrogen

The Effect of Carbonization Temperature on the Particle Characteristics

The visual appearance of dried lignin and carbonized lignin at temperatures of 500, 700, and 900 °C are shown in Fig. 2(a-d). The dried lignin has a brownish-red appearance and bulky form. Carbonized lignin is black and shiner with the increase in carbonization temperature caused by the decomposition of the organic compound of some lignin constituents into volatile gases and solid carbon. TG-DTA measurement has confirmed the disappearing of the organic compound during the carbonization by decreasing the weight percentage with increasing the temperature. To investigate further the functional groups existing in the dried lignin and the carbonized lignins in varied temperatures, FTIR analysis is carried out.

Fig. 3 represents the FTIR spectrum of dried lignin and carbonized lignin at temperatures of 500, 700, and 900 °C. The characteristics of FTIR spectrum of dried lignin corresponds to FTIR spectrum at wavenumbers: (1) 3338 cm^{-1} ; (2) 2920 cm^{-1} ; (3) 1695 cm^{-1} ; (4) 1604 cm^{-1} ; (5) 1509 cm^{-1} ; (6) 1420 cm^{-1} ; (7) 1213 cm^{-1} ; (8) 1112 cm^{-1} ; and

(9) 1033 cm^{-1} . These absorption bands in the FTIR spectrum can be assigned to (1) hydroxyl groups in phenolic and aliphatic structures, (2) CH stretching in aromatic methoxyl groups and in aliphatic methyl and methylene groups of side chains, (3) C=O stretching in conjugated *p*-substituted aryl ketones, (4) -C=O of pyruvate, (5) C=C stretching of the aromatic ring (G)CH deformation, (6) C-H asymmetric deformation in -OCH₃, (7) aromatic C-O stretching vibrations, (8) aromatic C-H in-plane deformation, and (9) C_{alkyl}-O ether vibrations methoxyl, respectively [21]. The spectra presented the characteristic peaks of lignin that also reported by others [22-23]. The functional groups of lignin are gradually removed with the increase of carbonization temperature. The pyruvate bond -C=O, the aromatic ring C=C, and the C_{alkyl}-O-ether methoxyl are still observed at the carbonization temperature of 500 °C. Most of the functional groups of lignin disappear at temperatures of 700 and 900 °C and approach the graphite spectrum.

XRD analysis is used to examine the change in the XRD pattern caused by the carbonization temperature.

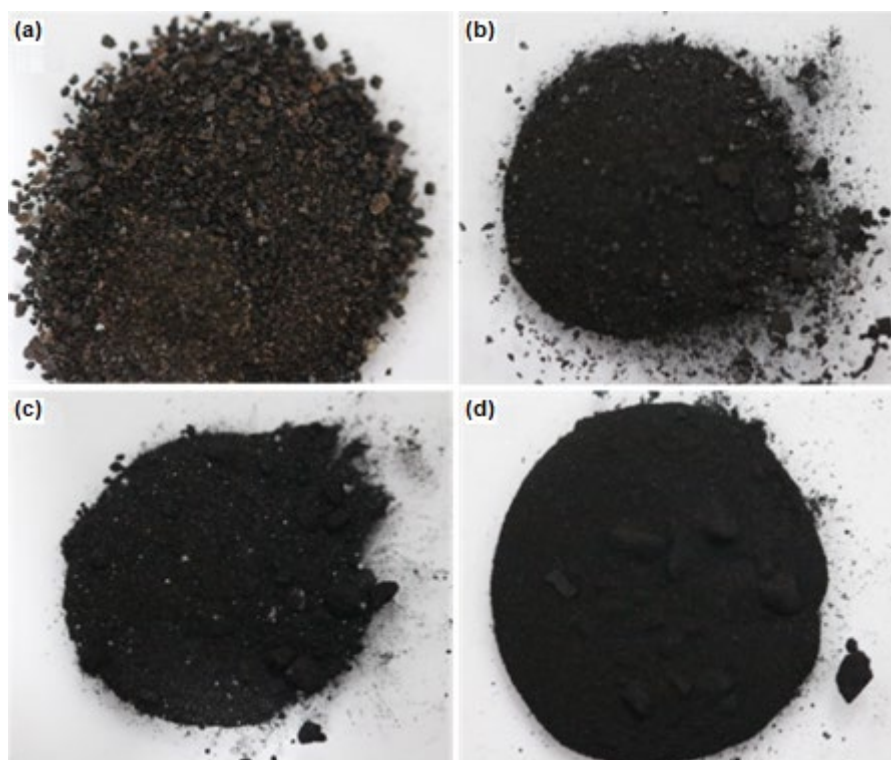


Fig 2. Visual appearances of (a) dried lignin, (b) carbonized lignin at 500 °C, (c) 700 °C, and (d) 900 °C

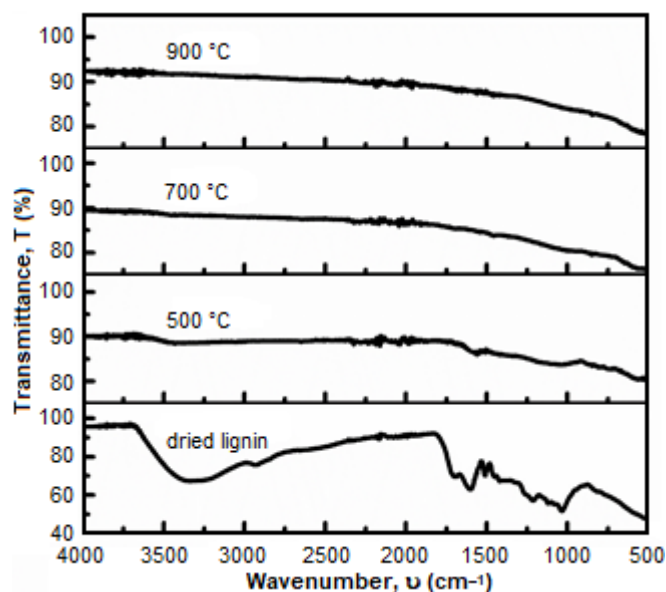


Fig 3. FTIR spectra of dried lignin and carbonized lignins at temperatures of 500, 700, and 900 °C

The XRD pattern of dried lignin and carbonized dried lignin at temperatures of 500, 700, and 900 °C are shown in Fig. 4. The plane of graphite structure (002) at the peak intensity 2θ centered at around 26.5° shows more clearly for carbonized lignin than that of the dried lignin. Increasing the carbonization temperature also slightly shifts the 2θ peak position of the plane (002) to the right position from 21.8° to 25.3° . However, for the carbonization at a temperature of 900 °C, the peak intensity 2θ of the plane (002) shifts back to the left to the position of 23.3° . Another 2θ peak intensity at around 44° is also observed for carbonized lignin and is not found in the dried lignin. The intensity is more apparent with the increase of the carbonization temperature. The same with the peak intensity 2θ of the plane (002), the peak intensity 2θ at around 44° corresponds to the plane (101), which is also assigned to the graphitic sheets. The presences of the broad profiles of the X-ray diffraction patterns represent that the structure of carbon materials is amorphous.

The effect of carbonization temperature on particle morphology is characterized by Scanning Electron Microscopy (SEM). SEM images for dried lignin and carbonized lignin at temperatures of 500, 700, and 900 °C are depicted in Fig. 5 (a-d). For low magnification, all samples exhibit shape irregularly and agglomerated

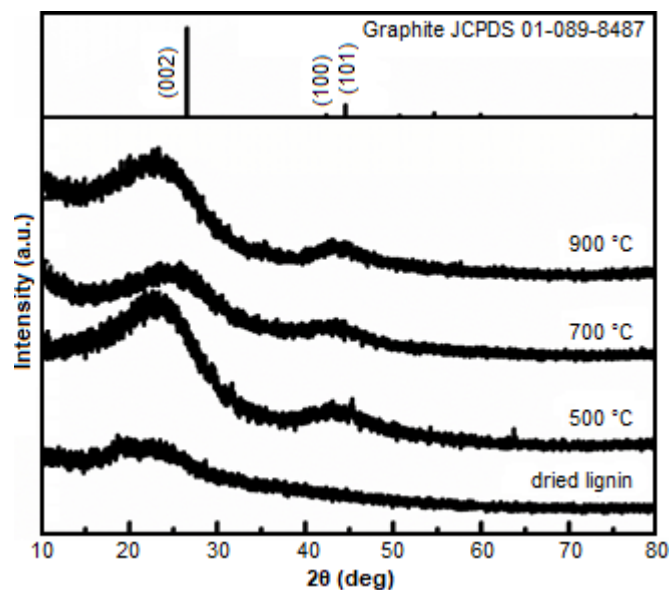


Fig 4. X-ray diffraction patterns of dried lignin and carbonized lignins at temperatures of 500, 700, and 900 °C

particles with the size of a few micrometers. However, for higher magnification (insets Fig. 5(a-d)), the distinct microstructures can be observed. For dried lignin, it can be shown that the agglomerated particles consisted of particles in the scale of nanometers. On the other hand, the size and the number of particle's pore increase with the increase in temperature, as shown in the high magnification SEM images. The increasing carbonization temperature led to the decomposition of more volatile components left behind the micro- and mesoporous carbon particles. The formation of pores for carbonized lignin brings out the increase in the specific surface area that will be explained in the following paragraph.

Table 1 shows the comparison of the specific surface area, pore diameter, and pore volume of lignin without carbonization and with carbonization at various temperatures. The surface area based on BET isotherm analysis of dried lignin extracted from the soda process of coconut coir without followed by carbonization was only $7.037 \text{ m}^2/\text{g}$. The carbonization at temperature of 500 °C increased the specific surface area of the sample to $157.621 \text{ m}^2/\text{g}$. An increase in carbonization temperature to 700 °C could make a 4-fold increase in the specific surface area compared to 500 °C. However, the specific surface area slightly decreased to $541.277 \text{ m}^2/\text{g}$ for the

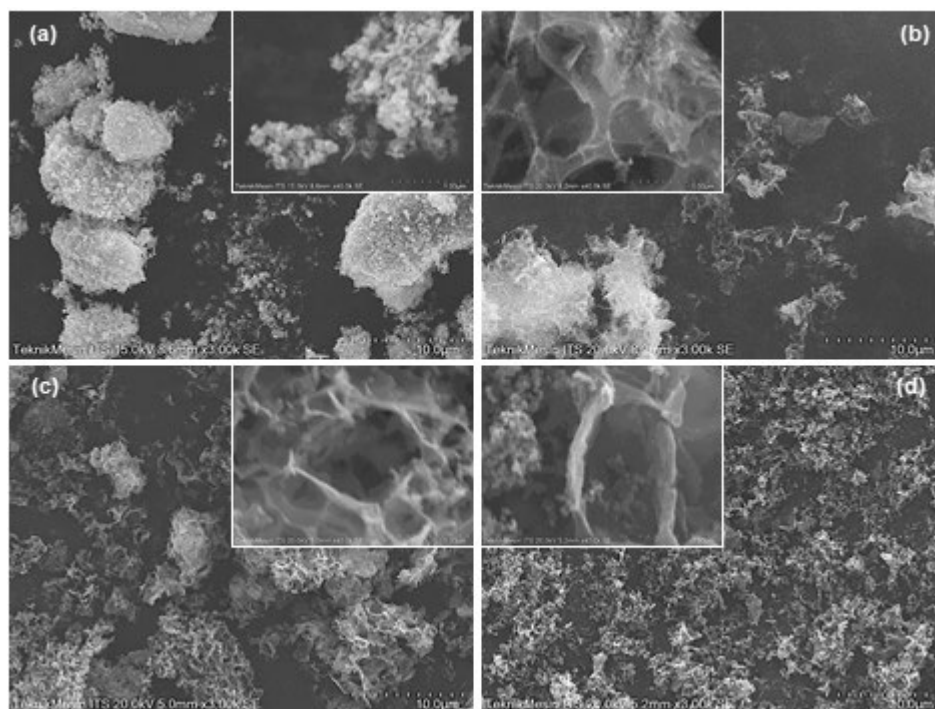


Fig 5. SEM images of (a) dried lignin, (b) carbonized lignins at 500 °C, (c) 700 °C, and (d) 900 °C

Table 1. Specific surface area, pore diameter, and pored volume of dried lignin and carbonized lignin at various temperatures

| Sample | Specific surface area (m ² /g) | Pore diameter (nm) | Pore volume (cm ³ /g) |
|--------------------------|--|-----------------------|-------------------------------------|
| Dried lignin | 7.037 | 3.433 | 0.002 |
| Carbonized lignin 500 °C | 157.621 | 3.841 | 0.013 |
| Carbonized lignin 700 °C | 642.501 | 3.387 | 0.050 |
| Carbonized lignin 900 °C | 541.277 | 3.407 | 0.084 |

carbonization at a temperature of 900 °C. The pore size for all samples was not so different, which was in the range of 3–4 nm categorized into mesopore type (2 nm < pore size < 50 nm). The pore volume increased with temperature in which lignin carbonized at 500, 700, and 900 °C had 7, 25, and 42 times more pore volume, respectively, compared to the dried lignin. The decomposition of the most functional group of lignin during carbonization left behind larger pore volume with relatively the same size pore for higher carbonization temperature.

The isothermal adsorption-desorption profiles as a function of the relative pressure of carbonization of lignin at temperatures of 700 and 900 °C are depicted in Fig. 6. Based on the IUPAC 1985 classification, the profiles of carbonized lignin at the temperatures of 700 and 900 °C

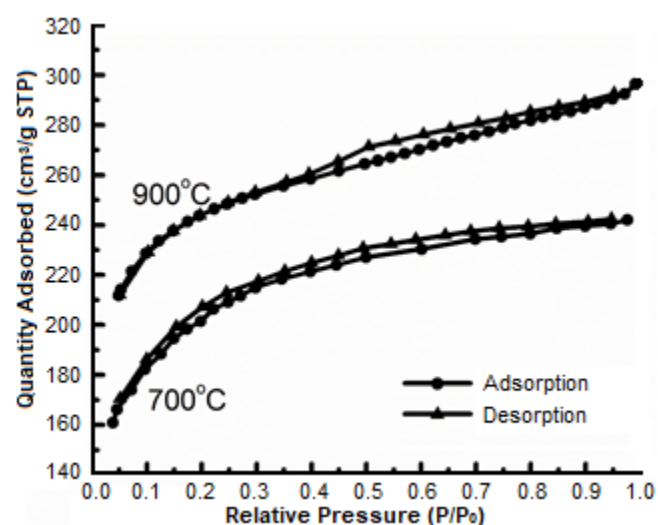


Fig 6. Adsorption and desorption isotherms of the lignin calcined at temperatures of 700 and 900 °C

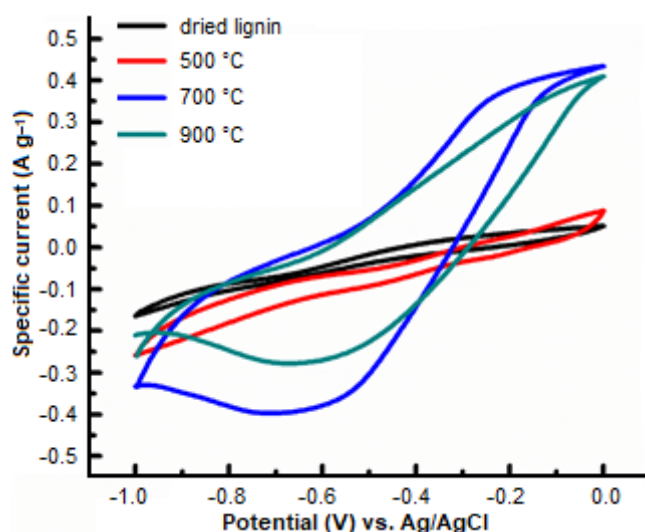


Fig 7. Voltammograms obtained in three-split electrode configuration at 10 mV/sec for dried lignin, carbonized lignin at various temperatures

can be categorized to the Type IV isotherm because there are hysteresis loops [24]. Even though the hysteresis is narrow, the hysteresis is associated with the filling and the emptying of the mesopores by capillary condensation.

The Electrochemical Properties

Fig. 7 shows the cyclic voltammetry curves of the samples at a 10 mV/sec sweep rate. The cyclic voltammetry did not exhibit rectangular curves as the behavior of the double layer capacitive material; however, the symmetry and un-peak curve can be obtained. The specific capacitance calculated using Eq. (1) for dried lignin, carbonized lignin 500 °C, carbonized lignin 700 °C and carbonized lignin 900 °C are 1.96, 4.13, 28.84, and 17.90 F/g, respectively. The carbonized lignin 700 °C gives the highest specific capacitance that correlates with the highest specific surface area. Hu and Hsieh were also reported that the highest surface area and pore volume resulted in the highest specific capacitance and suitable for supercapacitors fabrication [16].

CONCLUSION

Lignin was successfully extracted from the liquid waste of the soda delignification process of coconut coir via neutralization using a hydrochloric acid solution. The extracted lignin was carbonized at various temperatures and characterized using scanning electron microscopy

(SEM), X-Ray diffraction (XRD), Fourier transform infrared spectrometry (FTIR), nitrogen adsorption-desorption analyzer and cyclic voltammetry (CV). The results showed that the carbonization process led to an increase in the specific surface area of the generated carbon particles. The carbonized lignins had mesopores and amorphous graphitic structure with the highest surface area (i.e., 642.5 m²/g) and specific capacitance (i.e., 28.84 F/g) at carbonization temperature of 700 °C.

ACKNOWLEDGMENTS

Research Grant sponsored by Directorate of Research and Community Services, Directorate General of Strengthening Research and Development, Ministry of Research Technology and Higher Education, Republic Indonesia (No. 128/SP2H/PTNBH/DRPM/2018) is gratefully acknowledged. The authors also want to thank Mr. Fahmi Reza Wijanarko and Ms. Deninta Nur Iwana for their assistance in the experiments.

REFERENCES

- [1] Haghdan, S., Rennecker, S., and Smith, G.D., 2016, "Sources of lignin" in *Lignin in Polymer Composites*, Eds. Faruk, O., and Sain, M., Elsevier Inc., Oxford, 1–11.
- [2] Graichen, F.H.M., Grigsby, W.J., Hill, S.J., Raymond, L.G., Sanglard, M., Smith, D.A., Thorlby, G.J., Torr, K.M., and Warnes, J.M., 2017, Yes, we can make money out of lignin and other bio-based resources, *Ind. Crops Prod.*, 106, 74–85.
- [3] Norgren, M., and Edlund, H., 2014, Lignin: Recent advances and emerging applications, *Curr. Opin. Colloid Interface Sci.*, 19 (5), 409–416.
- [4] Naseem, A., Tabasum, S., Zia, K.M., Zuber, M., Ali, M., and Noreen, A., 2016, Lignin-derivatives based polymers, blends and composites: A review, *Int. J. Biol. Macromol.*, 93, 296–313.
- [5] Thakur, V.K., and Thakur, M.K., 2015, Recent advances in green hydrogels from lignin: A review, *Int. J. Biol. Macromol.*, 72, 834–847.
- [6] Laurichesse, S., and Avérous, L., 2014, Chemical modification of lignins: Towards biobased polymers, *Prog. Polym. Sci.*, 39 (7), 1266–1290.

- [7] Jin, W., Tolba, R., Wen, J., Li, K., and Chen, A., 2013, Efficient extraction of lignin from black liquor via a novel membrane-assisted electrochemical approach, *Electrochim. Acta*, 107, 611–618.
- [8] Kouisni, L., Holt-Hindle, P., Maki, K., and Paleologou, M., 2012, The LignoForce System™: A new process for the production of high-quality lignin from black liquor, *J. Sci. Technol. For. Prod. Processes*, 2 (4), 6–10.
- [9] Wang, G., and Chen, H., 2013, Fractionation of alkali-extracted lignin from steam-exploded stalk by gradient acid precipitation, *Sep. Purif. Technol.*, 105, 98–105.
- [10] Kim, D., Cheon, J., Kim, J., Hwang, D., Hong, I., Kwon, O.H., Park, W.H., and Cho, D., 2017, Extraction and characterization of lignin from black liquor and preparation of biomass-based activated carbon therefrom, *Carbon Lett.*, 22, 81–88.
- [11] Yahya, M.A., Al-Qodah, Z., and Ngah, C.W.Z., 2015, Agricultural bio-waste materials as potential sustainable precursors used for activated carbon production: A review, *Renewable Sustainable Energy Rev.*, 46, 218–235.
- [12] Seo, J., Park, H., Shin, K., Baeck, S.H., Rhym, Y., and Shim, S.E., 2014, Lignin-derived macroporous carbon foams prepared by using poly(methyl methacrylate) particles as the template, *Carbon*, 76, 357–367.
- [13] Balgis, R., Widiyastuti, W., Ogi, T., and Okuyama, K., 2017, Enhanced electrocatalytic activity of Pt/3d hierarchical bimodal macroporous carbon nanospheres, *ACS Appl. Mater. Interfaces*, 9 (28), 23792–23799.
- [14] Snowdon, M.R., Mohanty, A.K., and Misra, M., 2014, A study of carbonized lignin as an alternative to carbon black, *ACS Sustainable Chem. Eng.*, 2 (5), 1257–1263.
- [15] Rabinovich, M.L., Fedoryak, O., Dobeles, G., Andersone, A., Gawdzik, B., Lindström, M.E., and Sevastyanova, O., 2016, Carbon adsorbents from industrial hydrolysis lignin: The USSR/Eastern European experience and its importance for modern biorefineries, *Renewable Sustainable Energy Rev.*, 57, 1008–1024.
- [16] Hu, S., and Hsieh, Y.L., 2017, Lignin derived activated carbon particulates as an electric supercapacitor: Carbonization and activation on porous structures and microstructures, *RSC Adv.*, 7 (48), 30459–30468.
- [17] Correa, C.R., Stollovsky, M., Hehr, T., Rauscher, Y., Rolli, B., and Kruse, A., 2017, Influence of the carbonization process on activated carbon properties from lignin and lignin-rich biomasses, *ACS Sustainable Chem. Eng.*, 5 (9), 8222–8233.
- [18] Wang, H., Qiu, X., Liu, W., and Yang, D., 2017, Facile preparation of well-combined lignin-based carbon/ZnO hybrid composite with excellent photocatalytic activity, *Appl. Surf. Sci.*, 426, 206–216.
- [19] Vivekanandhan, S., Misra, M., and Mohanty, A.K., 2015, Microscopic, structural, and electrical characterization of the carbonaceous materials synthesized from various lignin feedstocks, *J. Appl. Polym. Sci.*, 132 (15), 41786.
- [20] Fauziyah, M., Widiyastuti, W., Balgis, R., and Setyawan, H., 2019, Production of cellulose aerogels from coir fibers via an alkali-urea method for sorption applications, *Cellulose*, 26, 9583–9598.
- [21] Raschip, I.E., Hitruc, E.G., and Vasile, C., 2011, Semi-interpenetrating polymer networks containing polysaccharides. II. Xanthan/lignin networks: A spectral and thermal characterization, *High Perform. Polym.*, 23 (3), 219–229.
- [22] do Santos, P.S.B., Erdocia, X., Gatto, D.A., and Labidi, J., 2014, Characterisation of Kraft Lignin Separated by Gradient Acid Precipitation, *Ind. Crops Prod.*, 55, 149–154.
- [23] Toledano, A., Serrano, L., Garcia, A., Mondragon, I., and Labidi, J., 2010, Comparative study of lignin fractionation by ultrafiltration and selective precipitation, *Chem. Eng. J.*, 157 (1), 93–99.
- [24] Rouquerol, J., Rouquerol, F., Llewellyn, P., Maurin, G., and Sing, K., 2014, *Adsorption by Powders and Porous Solids: Principles, Methodology and Applications*, 2nd Ed., Academic Press, London.